

Supporting Information

The Stability of Silver Nanoparticles in a Model of Pulmonary Surfactant

Leo Bey Fen,^{1,2} Shu Chen,¹ Yoshihiko Kyo,¹ Karla-Luise Herpoldt¹, Nicholas J. Terrill,³ Iain E. Dunlop,¹ David S. McPhail,¹ Milo S. Shaffer,³ Stephan Schwander,⁴ Andrew Gow,⁵ Junfeng (Jim) Zhang,⁶ Kian Fan Chung,⁷ Teresa D. Tetley,⁷ Alexandra E. Porter^{1*} and Mary P. Ryan^{1*}

¹Department of Materials and London Centre for Nanotechnology, Imperial College London, Exhibition Road, London SW7 2AZ, UK

²Department of Mechanical Engineering, Faculty of Engineering Building, University of Malaya, Kuala Lumpur 50603, MALAYSIA

³Department of Chemistry and London Centre for Nanotechnology, Imperial College London, Exhibition Road, London SW7 2AZ, UK

⁴Department of Environmental and Occupational Health, University of Medicine and Dentistry (UMDNJ) School of Public Health, New Jersey, USA

⁵Department of Pharmacology and Toxicology at Rutgers University, Piscataway, NJ, USA

⁶Department of Preventive Medicine, Keck School of Medicine, University of Southern California, USA

⁷National Heart and Lung Institute, Imperial College London, UK

Phases of DPPC

There are four lamellar phases recognised in saturated phosphatidylcholines (e.g. DPPC): a liquid-crystalline phase (L_α) and phases with ordered hydrocarbon chain arrangements, namely subgel or crystal phase (L_c), gel phase (L_β) and ripple phase (P_β).¹ The pretransition temperature associated with lamellar gel phase (L_β) to ripple phase (P_β) in aqueous dispersion of DPPC is approximately 35 °C. Whereas, the main transition temperature of gel-to-fluid phase is observed at 42 °C^{2, 3}. Below this transition or melting temperature, hydrated DPPC molecules are mobile but rotate occasionally.

Experimental Protocols

Synthesis of the AgNP suspension

AgNPs were synthesised by chemical bath reduction using sodium borohydride as the reductant and citrate as the stabiliser.⁴ Briefly, AgNO_3 ($\sim 1.0 \times 10^{-3}$ M) solution and $\text{Na}_3\text{C}_6\text{H}_5\text{O}_7$ ($\sim 1.0 \times 10^{-3}$ M) solution were added to boiling water (250 mL). Then, NaBH_4 solution ($\sim 1.0 \times 10^{-3}$ M) was added drop-wise to the mixture over a period of 10 seconds. The colour of the solution immediately turned to yellow, indicating the formation of silver particles. Heating was continued for an additional 30 minutes, and then the solution was cooled to room temperature. The AgNPs suspensions were washed with DI water and centrifuged at a relative centrifugal force maximum value (RCF_{max}) of 13,000 g. The washing process was repeated three times to remove impurities and unbound citrate. The final silver concentration after 3X washing with DI water was 23.5 ppm and all citrate was expected have been removed by the washing process. Then, these purified particles were sealed, stored in the dark and kept in a refrigerator. They were used within 2 weeks of sample preparation before diluting to 25mg/L in the DPPC pH solutions. The batch to batch variability of the AgNPs synthesis products is very low and all batches were routinely tested using TEM and

UV-vis measurements. The cleanliness of synthesised particles was confirmed with EDS to ensure that sulphidation of AgNPs had not occurred⁵ and impurities, such as Na⁺, Cl⁻ were removed by washing.

Transmission electron microscopy (TEM)

TEM was performed using a JEOL 2010 instrument operated at an accelerating voltage of 200 kV. The morphology and size distribution of AgNPs were characterised by bright field TEM. At least 200 particles were counted and measured to determine the size distribution (using Image J software). Two axes of particles (x and y) were calculated using Image J software as shown in Fig. S1. The particle size reported was estimated by averaging the shortest (x) and longest (y) dimension of 200 particles, *i.e.* $\left[\frac{x_k+y_k}{2}\right]$, $k = 0$ to 200 (SI). TEM samples were prepared by depositing a single drop of the suspension on to a 300 Cu Mesh holey support film and were left to dry at room temperature and stored under vacuum. To assess the effects of DPPC on the stability of the NPs, the samples were washed three times to remove excess organic surfactant, prior to TEM analysis. The samples were then negatively stained using 1% uranyl acetate in DI water to identify the phospholipid layer around AgNPs.⁶

Selected area electron diffraction (SAED)

The crystallinity of particles in different media was studied using SAED, in order to determine which phases were produced. In particular the possible presence of Ag, AgCl, Ag₂O or Ag₂S were determined by calculating the (111), (200) and (220) interplanar lattices and by comparing these to standard reference structures (Ag: Ref. # 01-087-0597; AgCl: Ref. # 00-031-1238; Ag₂O: Ref. # 00-041-1104; Ag₂S: Ref. # 00-014-0072).

Inductively Coupled Plasma–Optical Emission Spectroscopy (ICP-OES) was used to determine the amount of dissolved Ag in the test media. Post-incubation, each AgNP suspension was centrifuged at high speed (13,000 rpm) with 2 kDa (< 4 nm) filter tubes (Sartorius Stedim VIVACON 500) to separate the NPs from the solution. The concentration of released Ag⁺ ions was measured after the particles had been removed at different time intervals of 1, 6, 24, 72, 168 and 336 hours (n = 3). As a control, pure water (no AgNPs) and supernatant from which the the AgNPs had been removed were analysed, to ensure that any residual AgNPs were removed by centrifugation and filtering.

Zeta Potential Measurement. The surface charge (zeta potential) of AgNPs/citrate and AgNPs/citrate wrapped with a DPPC lipid layer were characterised with a ZetaPALS (Brookhaven Instruments Corporation, USA) as a function of pH and at 25 °C. The zeta potential measurements were calculated based on the electrophoretic mobility of charged particles in the dispersion (μ), viscosity (η) and permittivity (ϵ) of the solvent using the Smoluchowski equation: $\zeta = \frac{\mu\eta}{\epsilon}$, which determines the magnitude of the electrostatic repulsive force. The pH of the suspension was adjusted to the required value. The samples were sonicated for 2 minutes before making a measurement. The measurement was made in triplicate and the arithmetic mean reported.

Small Angle X-ray Scattering (SAXS) was performed on the I22 beamline at the Diamond Light Source to provide an in-situ correlative measure of particle size and aggregation state. SAXS measurements were performed on the I22 beamline at the Diamond Light Source. A beam energy of 13 keV and a low noise Pilatus 2M detector were used. A camera length of 4.3m gave an accessible q-range of 0.0437 to 0.3913 Å⁻¹. The scattering vector q describes the

difference between the wavevectors of the incident and diffracted beams. The detector was calibrated using Silver Behenate before the 2D detector image was integrated over 360° with a fixed radius and then normalised to give 1D data which were then adjusted for background scattering. Data reduction was performed using the Non-Crystalline Diffraction toolbox within Dawn Science (*Dawn Science*, <http://www.dawnscience.org>). Data modelling and fitting was carried out using SasView (ref. *SasView*, <http://www.sasview.org>). Data were fitted using a unified Guinier-Porod fit allowing the radius of gyration (R_g) to be extracted as well as information about the particle dimensionality⁷. Fits with a dimension <0.25 were assumed to be spherical and the particle diameter was calculated using the equation $D = 2R_g \left(\frac{3}{5}\right)^{-\frac{1}{2}}$.

AgNP were diluted to a concentration of 10 µg/ml. As-prepared NPs were measured in 1 mm quartz capillaries using a 120 s exposure time. DPPC at 10 µg/ml was added to each pH solution. Samples were then incubated in a water bath at 37°C for 560 minutes (~9.5 hours) before being measured in the X-ray beam.

Supporting Figures and Tables

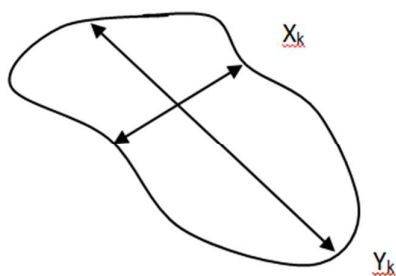


Figure S1: Schematic diagram showing the procedure used to measuring the particle size.

The particle size reported was estimated by averaging the shortest (X)

dimension of 200 selected particles, *i.e.* $\left[\frac{x_k+y_k}{2}\right]$, $k=1$ to 200.

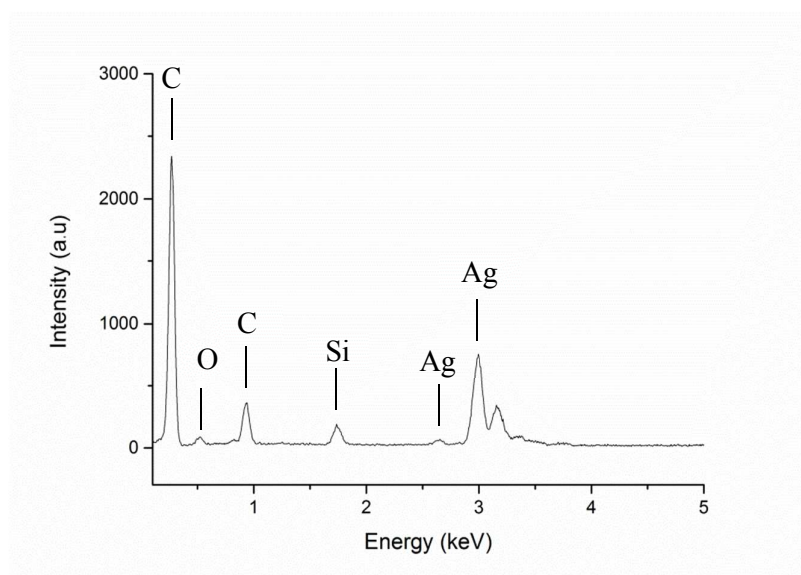


Figure S2. EDS spectrum of as – synthesised 20 nm AgNPs.

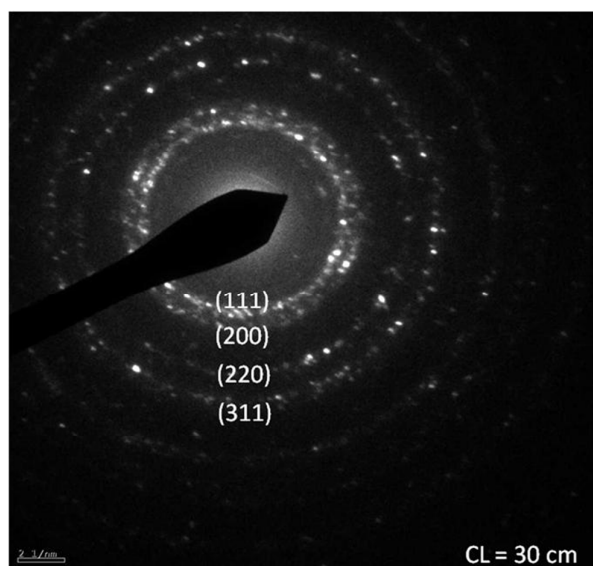


Figure S3. Indexed selected area electron diffraction (SAED) patterns of AgNPs incubated in DI water. The selective aperture size used was 100 nm in diameter.

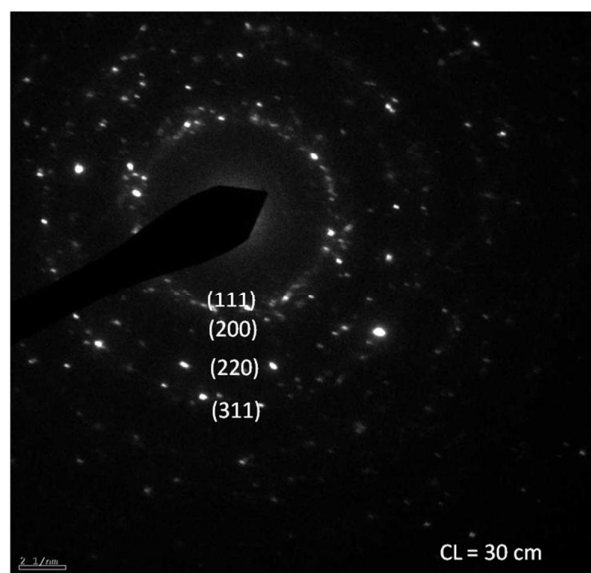


Figure S4. Indexed SAED patterns of AgNPs incubated in pH 3 solutions without DPPC for 1 week. The selective aperture size used was 100 nm in diameter.

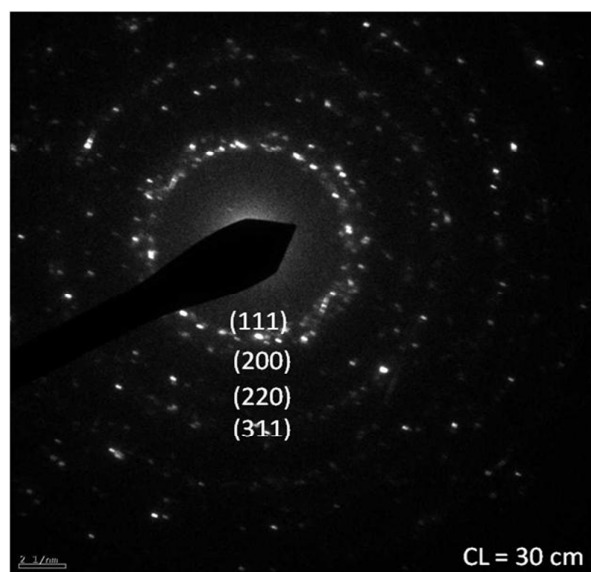


Figure S5. Indexed SAED patterns of AgNPs incubated in pH 3 solutions with DPPC for 1 week. The selective aperture size used was 100 nm in diameter. characteristic spacings of metallic silver are observed; any other crystalline phases, such as chlorides, oxides, or sulphides were either absent or present in negligible concentration.

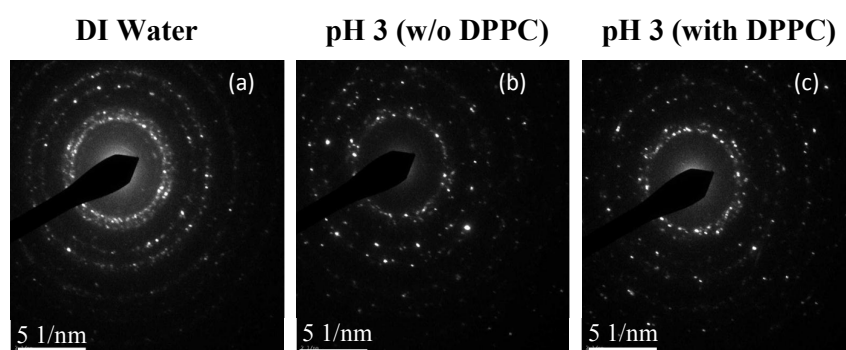


Figure S6. SAED patterns taken from aggregates of AgNPs incubated for 1 week in (a) DI water, (b) pH 3 solution without DPPC, and (c) with DPPC. The selective area aperture size used was 100 nm in diameter. (Indexed patterns are shown in S1, S2 and S3).

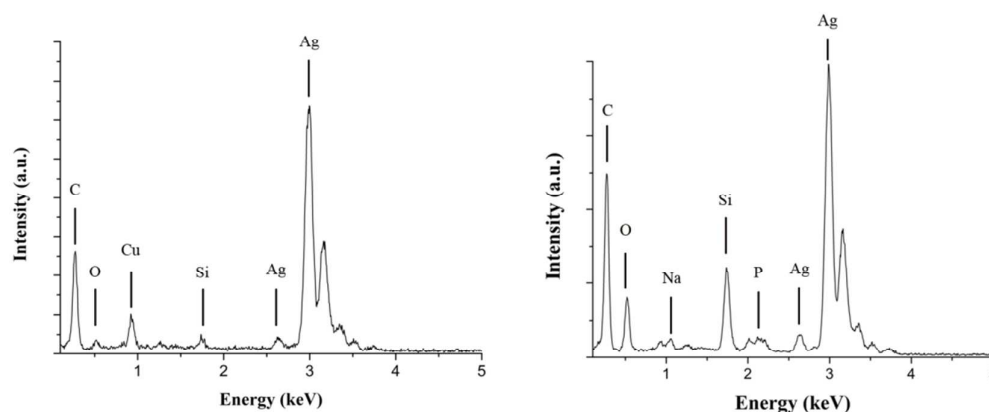


Figure S7. EDX spectra taken from AgNPs incubated in pH3 solution, (a) in the absence, and (b) in the presence of DPPC, for 1 week.

Table S1. The lattice parameter of samples as a function of pH and incubating medium (with and without DPPC).

h k l	Ag (Standard)	AgNPs 20 nm	<u>with DPPC</u>			<u>without DPPC</u>		
			pH3	pH5	pH7	pH3	pH5	pH7
1 1 1	0.236	0.230	0.235	0.235	0.231	0.241	0.232	0.234
2 0 0	0.204	0.202	0.199	0.202	0.203	0.208	0.201	0.201
2 2 0	0.145	0.142	0.121	0.143	0.142	0.149	0.143	0.144
Lattice constant (nm)	0.409	0.402	0.402	0.406	0.401	0.410	0.403	0.403

References

1. Leonenko, Z. V.; Finot, E.; Ma, H.; Dahms, T. E. S.; Cramb, D. T., Investigation of temperature-induced phase transitions in DOPC and DPPC phospholipid bilayers using temperature-controlled scanning force microscopy. *Biophysical Journal* **2004**, *86*, (6), 3783-3793.
2. Tristram-Nagle, S.; Nagle, J. F., Lipid bilayers: thermodynamics, structure, fluctuations, and interactions. *Chemistry and Physics of Lipids* **2004**, *127*, (1), 3-14.
3. Rappolt, M.; Rapp, G., Structure of the stable and metastable ripple phase of dipalmitoylphosphatidylcholine. *European Biophysics Journal with Biophysics Letters* **1996**, *24*, (6), 381-386.
4. Solomon, S. D.; Bahadory, M.; Jeyarajasingam, A. V.; Rutkowsky, S. A.; Boritz, C.; Mulfinger, L., Synthesis and study of silver nanoparticles. *Journal of Chemical Education* **2007**, *84*, (2), 322-325.
5. Levard, C.; Hotze, E. M.; Lowry, G. V.; Brown, G. E., Environmental Transformations of Silver Nanoparticles: Impact on Stability and Toxicity. *Environmental Science & Technology* **2012**, *46*, (13), 6900-6914.
6. De Carlo, S.; Harris, J. R., Negative staining and cryo-negative staining of macromolecules and viruses for TEM. *Micron* **2011**, *42*, (2), 117-131.
7. Hammouda, B., A new Guinier-Porod model. *Journal of Applied Crystallography* **2010**, *43*, 716-719.